[3]Joslin, R. D., Streett, C. L., and Chang, C.-L., "Validation of Three-Dimensional Incompressible Spatial Direct Numerical Simulation Code—A Comparison with Linear Stability and Parabolic Stability Equations Theories for Boundary-Layer Transition on a Flat Plate," NASA TP-3205, July 1992.

[4]Joslin, R. D., Streett, C. L., and Chang, C.-L., "Spatial DNS of Boundary-Layer Transition Mechanisms: Validation of PSE Theory," *Theoretical Computational Fluid Dynamics*, Vol. 4, No. 6, 1993, pp. 271–288.

[5]Williamson, J. H., "Low-Storage Runge–Kutta Schemes," *Journal of Computational Physics*, Vol. 35, No. 1, 1980, p. 48.

[6]Danabasoglu, G., Biringen, S., and Streett, C. L., "Spatial Simulation of Instability Control by Periodic Suction and Blowing," *Physics of Fluids*, Vol. 3, No. 9, 1991, pp. 2138–2147.

[7]Streett, C. L., and Hussaini, M. Y., "A Numerical Simulation of the Appearance of Chaos in Finite-Length Taylor-Couette Flow," *Applied Numerical Mathematics*, Vol. 7, No. 1, 1991, p. 41.

[8]Streett, C. L., and Macaraeg, M. G., "Spectral Multi-Domain for Large-Scale Fluid Dynamic Simulations," *Applied Numerical Mathematics*, Vol. 6, No. 1–2, 1989/1990, p. 123.

Application of Similarity in Hypersonic Transition Prediction

Alexander V. Fedorov* and Norman D. Malmuth†
Rockwell International Science Center, Thousand Oaks, California 91358

Introduction

PREDICTION of laminar-turbulent transition in hypersonic boundary layers is of critical importance for aircraft and missile design.[1] Although considerable effort has been invested in developing theoretical and computational methods to predict high Mach number transition, a strong need still exists for approaches suitable for rapid response design application. To fill this need, empirical criteria based on wind tunnel and flight experiments are currently the main workhorses in engineering practice. Much of the difficulty in constructing a rapid design oriented method is due to the unique features of the hypersonic stability and transition problem that include strong nonparallelism and shock effects. In spite of the success of e^N methods such as those in Ref. 2 below Mach 12, these aspects are significant at higher Mach numbers.

In this Note, similarity methods will be used to indicate a new, potentially useful procedure for preliminary design and fast tradeoff studies. These methods have the potential of dealing with some of these difficulties. The theoretical basis for the similarity method will be given and an application to hypersonic cones provided. Finally, possibilities for generalization of the method to more arbitrary shapes will be discussed.

Since the problem of disturbance evolution contains the large Mach and Reynolds number parameters, it is natural to use asymptotic methods in predictive models. Asymptotic theories for the vorticity mode, crossflow instability Gortler vortices, and the analysis of Ref. 3 are recent examples. Solutions from this class of asymptotic models are limited in their applicability because of the restrictive asymptotic limit processes used. Other asymptotic approximations provide more general applicability but are also more difficult to solve. Even without solution, however, such theories give important similarity groups, if appropriate normalizations and nondimensionalizations are used that reflect the salient phenomenological scales. These groups provide the basis for constructing similarity laws that can be useful not only for design of economical experiments but also for prediction as well.

Such a procedure will be used in this paper to investigate similitude of boundary-layer stability over nearly sharp, zero-incidence hypersonic cones. A similarity rule accounting for viscous and compressibility effects is derived without solving the initial boundary value problem. Predictions from the rule are compared with linear stability computations as well as (re-entry F) flight data obtained on slender cones.[4] It will be seen that this rule gives an extremely cost-effective and rapid extrapolation method of code or experimentally derived data to other conditions.

Similarity Analysis

The unsteady disturbance field in a three-dimensional hypersonic boundary layer will be considered with the following assumptions. 1) The fluid is a perfect gas with constant Prandtl number Pr and specific heat ratio γ. Denoting starred quantities as dimensional, the viscosity–temperature law is $\mu^* = \mu_0^* T^{*\omega}$. 2) The spatial scales of the disturbances are of the order of boundary-layer displacement thickness δ^*; the time scale is δ^*/U_e^*, where subscript e refers to the upper edge of the boundary layer. 3) Boundary-layer disturbances weakly interact with the external inviscid flow and shock wave.

In the hypersonic boundary layer, the pressure is of the order of that of the external inviscid flow, and the temperature is of the order of the stagnation temperature $T_s^* \sim (\gamma - 1)M_e^2 T_e^*$. This leads to asymptotic scaling for the flow variables within the boundary layer. The full Navier–Stokes equations written in terms of this scaling contain only the lumped parameter $R = \varepsilon^{1+\omega} Re$, where $\varepsilon \equiv 1/[(\gamma - 1)M_e^2] \ll 1$ and Re is the Reynolds number based on the displacement thickness, $Re = \delta^* U_e^* \rho_e^*/\mu_e^*$. The dependence on the similarity parameter R is valid for strong, moderate, and weak viscous-inviscid interaction regimes. However, δ^* and, as a result, the Reynolds number Re are sensitive to the interaction type. For example, the boundary layer on a flat plate has the displacement thickness $\delta^* \sim x^{*3/4}$ for strong interaction and $\delta^* \sim x^{*1/2}$ for a weak one.

Outside the boundary layer, the disturbances are assumed to vanish and weakly interact with the external inviscid flow. At the wall, the flow satisfies no-slip conditions, and temperature is assumed to be constant. The upstream and downstream conditions as well as initial conditions for the disturbances are also assumed to depend weakly on Mach and Reynolds number. These additional provisions preserve the applicability of the R similitude previously indicated. It is therefore clear that the similarity law

$$f = fn(R, \gamma, T_f, Pr) \tag{1}$$

holds, where f is any of the flow-dependent variables, T_f is the wall temperature ratio, and fn signifies a functional dependence that can be obtained from solution of the initial value problem.

This similarity can be extended to the linear stability problem if a typical eigenmode wavelength λ^* is of the order of the boundary-layer thickness. If small disturbances are assumed in the original form of the Navier–Stokes equations before the previously mentioned rescaling is used, the general linearized equations (LSE) for small fluctuations are obtained. Within the spatial and temporal scaling implied by the wavelength assumption, the equations for the fluctuations depend again only on the parameters γ, T_f, Pr, and R if further, their initial and boundary conditions are consistent with this assumption. Therefore, the fluctuations obey a similarity law such as Eq. (1).

As an example, consider the two-dimensional vorticity mode (second mode according to Mack's classification[5]) in the boundary layer on a flat plate or sharp cone. In this case, the span component of the wave vector $\beta = 0$ and the growth rate $\sigma = -\mathrm{Im}(\alpha)$ (where $\alpha =$ the complex eigenvalue). If the Prandtl number, specific heat ratio, and viscosity exponent parameters Pr, γ, and ω, as well as the wall temperature factor $T_f = T_w^*/T_{ad}^*$, are fixed, where T_w^* is the wall temperature, and T_{ad}^* is the adiabatic wall temperature, the maximum growth rate $\sigma_m(\Omega)$ ($\Omega = \Omega^* \delta^*/U_e^*$ the nondimensional frequency), is a function of Reynolds number Re and Mach number M_e.

In Fig. 1, calculations for σ_m from a linear stability code are shown as a function of the similarity parameter R at $M_e = 7$, 8, 10, 12, and

Received July 23, 1994; revision received Feb. 2, 1995; accepted for publication Feb. 2, 1995.

*Consultant; also Principal Researcher, Moscow Institute of Physics and Technology, 16 Gagarin Street, 140160 Zhukovsky, Russia.

†Project Manager, Computational Fluid Dynamics, 1049 Camino Dos Rios. Fellow AIAA.

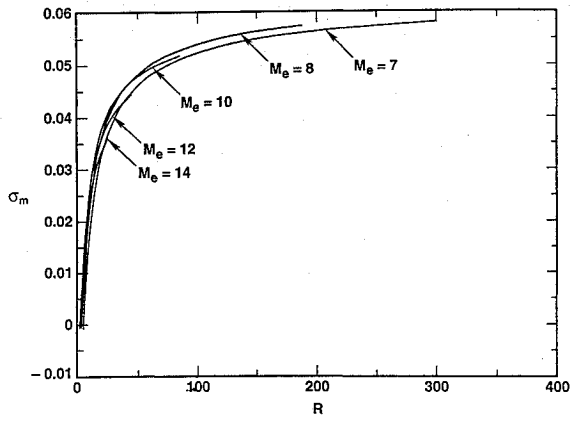

Fig. 1 Maximum growth rate as a function of similarity parameter R at various local Mach numbers M_e.

14. The following parameters were used in the computations: $Pr = 0.72$, $\gamma = 1.4$, $T_f = 0.2$, and $\omega = 0.75$. The stability characteristics were computed by solving the eigenproblem for the LSE system of equations.[5] In this procedure, the mean flow in the boundary layer was approximated by the hypersonic weak interaction theory self-similar solution. Note that the similarity given by Eq. (1) collapses the $\sigma_m(Re, M_e)$ curves to $\sigma_m(R)$ at moderate values of R, as Mach number increases. At sufficiently large R, the curves tend to spread, because the wavelength of the vorticity mode $\lambda^* \ll \delta^*$ and assumption 2) is violated. This is consistent with the asymptotic theory for inviscid disturbances according to which the vorticity mode is concentrated in a thin transitional layer at the upper edge of the boundary layer. However, the region where similarity works well is sufficiently wide and relates well to practical applications.

Application of Similarity in Hypersonic Transition Prediction

Hypersonic cones are used as a focus to explore the use of similarity in transition prediction herein. Reference 4 provides transition data for a slender cone at freestream Mach number 20 during re-entry from altitudes of approximately 30.480 to 18.288 km, corresponding to the region of freestream Reynolds number 6.56 to 52.5×10^6 per meter. Experimental points representing transition onset Reynolds numbers $Re_{x,\mathrm{tr}} = U_e^* x_{\mathrm{tr}}^* / \nu_e^*$ (ν_e^* = kinematic viscosity), as a function of local Mach number M_e are shown by the symbols in Fig. 2. In the figure, I denotes the sharp cone, II signifies entropy layer swallowed by the boundary layer close to the transition location, and III represents swallowing downstream of transition. The similarity relation Eq. (1) applies for regimes I and III.

Because of recession of the nose tip during re-entry, the local Mach number at the upper edge of the boundary layer depends on the nose-radius history. The maximum M_e corresponds to a sharp nose. As the tip is blunted, the boundary layer grows in a higher entropy gas with smaller local Mach number. The transition Reynolds number depends on the location of the region where the entropy layer is swallowed by the boundary layer.

More details are given in Ref. 6 of how this physics is related to the change in the monotonic trend of the regime III data shown in Fig. 2. For regime II, only local similarity rather than the global similarity (1) is valid that is associated with almost constant boundary-layer edge flow quantities. The latter corresponds to sharp cone similitude at a given local Mach number. For this case, the flat plate mean flow viscous interaction parameter $\chi \equiv (\gamma - 1)M_e^3\sqrt{Re_x}$ ($Re_x \equiv U_e^* x^* / \nu_e^*$), derived in Ref. 7 is related to transition onset. The assumption of weak interaction $\chi \ll 1$ is well satisfied by experimental data of Ref. 4. From Ref. 7, and application of the Blasius formula locally, the boundary-layer displacement thickness δ^*, local Reynolds number Re, and similarity parameter R are

$$\delta^* = \varepsilon^{-\frac{1+\omega}{2}} \Delta \sqrt{\mu_e^* x^* / \rho_e^* U_e^*} \tag{2}$$

$$Re = \Delta \varepsilon^{-\frac{1+\omega}{2}} \sqrt{Re_x}, \qquad R = \Delta \varepsilon^{\frac{1+\omega}{2}} \sqrt{Re_x} \tag{3}$$

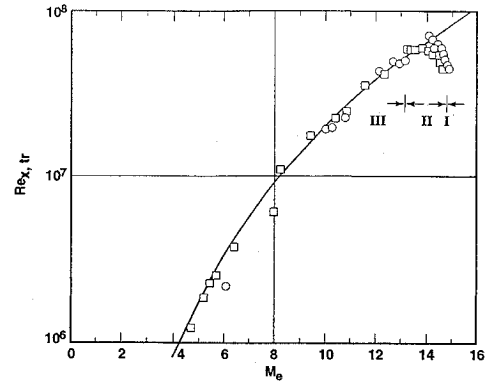

Fig. 2 Comparison of present theory with flight experiment.

using the perfect gas law, energy invariant, and the previously stated viscosity-temperature law, where $\Delta \equiv$ the constant of proportionality in this law.

In Eqs. (2) and (3), Δ is a weak function of M_e. In the hypersonic limit, Δ is assumed independent of M_e. This approximation simplifies the prediction of the transition onset location that can be estimated by the e^N method. The amplification factor N for the two-dimensional second mode can be represented solely as a function of the similarity parameter R as

$$N(\Omega, x^*) \equiv \int_{x_0^*}^{x^*} \sigma^* \mathrm{d}x^* = \frac{2}{\Delta^2} \int_{R_0}^{R} \sigma \mathrm{d}R$$

where $\sigma^* = \sigma \delta^*$. Applying the transition onset criterion $N = N_{\mathrm{cr}}$, where N_{cr} is the critical amplification factor that is assumed to be a constant for regime III data from Ref. 4, the corresponding similarity parameter R_{tr} can be obtained. According to Eq. (3), $Re_{x,\mathrm{cr}} = \varepsilon^{-(1+\omega)} \Delta^{-2} R_{\mathrm{tr}}^2$. Since N_{cr} equals the constant independent of Mach number M_e and from $N = N_{\mathrm{cr}}(R)$, R_{tr} also equals the constant independent of Mach number M_e. Therefore, the similarity rule

$$\frac{(Re_{x,\mathrm{tr}})_1}{(Re_{x,\mathrm{tr}})_2} = \left(\frac{M_{e1}}{M_{e2}} \right)^{2(\omega+1)} \tag{4}$$

is obtained on use of the definition of ε and the fact that the other parameters are fixed.

Equation (4), shown in Fig. 2 as a solid line for $\omega = 0.75$, agrees excellently with flight data and provides a useful prediction tool that can be applied for other zero incidence cones. With Eq. (4), characteristics at new Mach numbers can be obtained from computed or experimental points corresponding to a particular cone geometry and wall-to-freestream temperature ratio.

Discussion, Future Work, and Conclusions

Efforts are under way to extend the applicability of the similarity method to more general shapes than cones and treat angle of attack cases. In this connection, it should be noted that similarity gives a relation between the local characteristics of the boundary layer. The simple form of the similarity rule, Eq. (4), was obtained under the assumption that the mean flow parameters at the boundary-layer edge are constant. Similarity appears also to be valid for transition due to some local process that is typical of nonlinear bypass mechanisms. If transition depends on the disturbance streamwise history and the mean flow has a nonuniform distribution in the x–z plane, similarity can be used to relate disturbance characteristics between two streamwise stations and account for the global process leading to transition. From the e^N method, the growth rate σ can be extrapolated to the new set of conditions at each point using similitude. This can be used to determine the amplification rate N to predict the transition Reynolds number. Since this approach would be derived under the other general conditions used here, it would be applicable not only for more complicated geometries but also for linear and nonlinear regimes as well.

Acknowledgment

A portion of this work was sponsored by the United States Air Force Office of Scientific Research under Contract F49620–92-C-0006.

References

[1]Malik, M., Zang, T., and Bushnell, D., "Boundary Layer Transition in Hypersonic Flows," AIAA Paper 90-5232, Oct. 1990.

[2]Fedorov, A. V., Gushchin, V. R., and Tumin, A. M., "Transition to Turbulence on Hypersonic Vehicles," *Proceedings of the ASME Fluid Engineering Conference* (Washington, DC), *Turbulent Flows—1993*, FED-Vol. 155, American Society of Mechanical Engineers, 1993, pp. 55–58.

[3]Malmuth, N. D., "Stability of the Inviscid Shock Layer in Strong Interaction Flow over a Hypersonic Flate Plate," *Instabilities and Turbulence in Engineering Flows*, Fluid Mechanics and Its Applications Series, Kluwer, Dordrecht, The Netherlands, 1993, pp. 189–223.

[4]Wright, R. L., and Zoby, E. V., "Flight Boundary Layer Transition Measurements on a Slender Cone at Mach 20," AIAA Paper 77-719, June 1977.

[5]Mack, L. M., "Boundary Layer Stability Theory," Jet Propulsion Lab., Doc. 900-277, Rev. A, Pasadena, CA, 1969.

[6]Fedorov, A., and Malmuth, N., "Analysis of Similarity Methods in Hypersonic Transition Prediction," Rockwell International Science Center, Rept. RISC94NM2, Thousand Oaks, CA, Aug. 1994.

[7]Hayes, W. D., and Probstein, R. F., *Hypersonic Flow Theory*, Academic, New York, 1959.

Vortex Development over Flat Plate Riblets in a Transitioning Boundary Layer

J. A. Rothenflue* and P. I. King†
U.S. Air Force Institute of Technology, Wright–Patterson Air Force Base, Ohio 45433

Introduction

THE majority of riblet research has focused on the reduction of turbulent boundary layer (TBL) skin-friction drag on a flat plate at zero pressure gradient.[1] For example, Choi[2] showed that riblets constrain the spanwise movement of the longitudinal vortices that exist just above the laminar sublayer. Current research by the authors is aimed at investigating potential applications for riblets in other than turbulent boundary layers.

For this research, riblets were placed in an incompressible, flat plate, zero-pressure-gradient boundary layer developing from a laminar to turbulent state. A three-component laser-Doppler anemometer was used to obtain velocity profiles within and above the riblets at several streamwise locations. Results indicate that riblets initiate the development of paired, streamwise vortices during boundary-layer transition. These vortices remain in place as they extend downstream and appear to evolve into the TBL vortical structures detected by Suzuki and Kasagi.[3]

Experimental Setup

The wind tunnel for this investigation consists of an air supply system, stilling chamber, and an enclosed test section that exhausts into a vented room. A flat test plate splits the test section from top to bottom, creating two separate 8 × 40 cm channels. Outer test section walls are adjustable to allow a zero pressure gradient along the length of the center plate. The freestream turbulence intensity entering the test section varies from 1.0 to 1.7%, depending on the freestream velocity.

Received Sept. 26, 1994; revision received March 31, 1995; accepted for publication April 3, 1995. This paper is declared a work of the U.S. Government and is not subject to copyright protection in the United States.

*Doctoral Candidate, ENA433. Member AIAA.

†Associate Professor, ENY, 2950 P Street. Senior Member AIAA.

V-groove riblets used for this investigation were machined into the Plexiglas test plate with 3.0-mm peak-to-peak width and 2.6-mm valley-to-peak height. The local u velocity component is defined parallel to the test plate in the streamwise direction, the v component normal to and away from the plate, and the w component parallel to the plate in the cross-stream direction, consistent with a right-handed coordinate system.

A DANTEC fiber flow three-axis laser-Doppler anemometry system was used in cross-coupled mode (off-axis backscatter), resulting in an approximately ellipsoidal probe volume measuring roughly 150 × 150 × 215 μm in size.

Results

Boundary-layer profiles were obtained over riblet valleys and peaks. In addition, spanwise velocity profiles over two riblets were taken at stations 0.5 and 3.0 mm above the riblet peaks. All profiles were obtained for three freestream velocities ($U \cong 3.5$, 7.5, and 15.0 m/s) and five streamwise stations on the plate ($x = 105$, 200, 300, 400, and 500 mm from the leading edge).

The state of the boundary layer (laminar, transitional, or turbulent) was determined from the distribution of turbulence intensity, given by $Tu = [(u_{\text{rms}}^2 + v_{\text{rms}}^2 + w_{\text{rms}}^2)/3]^{1/2} \times (1/U)$, as illustrated in Fig. 1. For the laminar boundary layer at $x = 105$ mm, the difference in turbulence intensity between the boundary layer and the freestream was negligible. In the transitional boundary layer at $x = 300$ mm, the elevated peak turbulence intensity within the boundary layer increased in the streamwise direction, until, for the fully turbulent boundary layer at $x = 500$ mm, the peak turbulence intensity remained constant. The arithmetic mean of two separate rms estimates, each based on 1000 Doppler bursts, was used to obtain Tu. For $U \cong 7.5$ m/s in Fig. 1, transition was first detected at $x = 200$ mm and was complete at $x = 400$ mm. For $U \cong 15.0$ m/s, transition began at $x \cong 105$ mm and was complete at $x = 400$ mm. Both of these cases correspond well with transition criteria given by Granville.[4] For the $U \cong 3.5$ m/s case however, transition began at $x \cong 300$ mm, earlier than the Granville prediction, and remained transitional up to the test section exit at $x = 500$ mm.

For all velocities, a pair of counter-rotating vortices developed within the riblet valleys downstream of initiation of transition. For this work, the vortices were first detected at $x = 500$ mm for $U \cong 3.5$ m/s, $x = 300$ mm for $U \cong 7.5$ m/s, and $x = 200$ mm for $U \cong 15.0$ m/s. Figures 2–4 include measurements at $x = 300$ mm, a location of transitional flow for all cases. At this x station, the 99% boundary-layer thickness was approximately 5.5 mm above the riblet peaks for $U \cong 3.5$ m/s and 4.5 mm for both $U \cong 7.5$ and 15.0 m/s. In these figures, each point is the arithmetic mean of the data from two passes, and each individual mean velocity measurement is the residence time-weighted mean of 1000 Doppler bursts. The 90% confidence intervals in the figures are based on the observed scatter in the data from the two passes and are representative for all data in the figure. Velocity confidence intervals never exceed ±0.4% of the freestream velocity.

Figure 2 shows the v velocity profiles over a riblet peak and valley, with the y datum at the bottom of the valley. It depicts a region of ascending particles above the peak and descending particles within the valley for $U \cong 7.5$ m/s and 15.0 m/s. Figures 3 and 4 are spanwise v and w profiles, respectively, spanning two complete riblets 0.5 mm

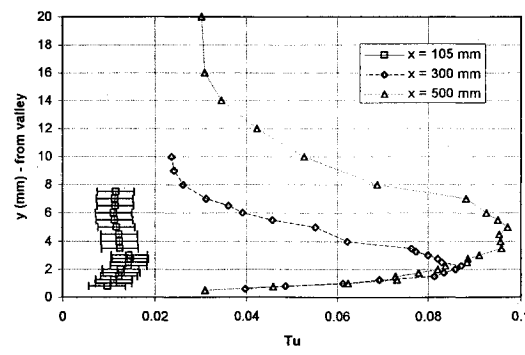

Fig. 1 Boundary layer Tu profiles, $U = 7.5$ m/s.